ELSEVIER

Chemical Engineering Journal 92 (2003) 169–176

Chemical Engineering Journal

www.elsevier.com/locate/cej

On the rise velocity of an interactive bubble in liquids

Jian Zhang [a,*], Liang-Shih Fan [b]

[a] *Department of Engineering Mechanics, Tsinghua University, Beijing 100084, China*
[b] *Department of Chemical Engineering, The Ohio State University, Columbus, OH 43210, USA*

Accepted 23 July 2002

Abstract

Bubble rise velocity is one of the important parameters characterizing bubble column systems. Mathematical models for predicting the velocity of an interactive spherical bubble rising in-line in liquids for intermediate Reynolds number range [*Re* ∼O(100)] are developed in the present study. The equation for the balance of forces on a bubble rising in-line is formulated. The models are derived based on this equation and different assumptions for the forces on the bubble. The ratios of the rise velocity of the trailing bubble to that of an isolated bubble, varying with the separation distance between the leading and trailing bubbles, are predicted by these models at *Re* of 35.4, 21.5 and 3.06. Comparisons between the predictions and the measurements show that the model incorporating both the wake effect and the bubble acceleration effect which includes the added mass and Basset forces can well predict the rise velocity of the trailing bubble in the far wake region of the leading bubble. The commonly used model which accounts for only the wake effect is found to lead to an overestimation of the rise velocity of the trailing bubble.

Keywords: Bubble–liquid systems; Bubble rise velocity; Bubble wake; Bubble–bubble interaction; Basset force

1. Introduction

Bubble columns are commonly encountered in chemical, petrochemical, biochemical, metallurgical, environmental, and other processing applications. The investigations of the hydrodynamic behavior of bubble columns involve both the macroscopic or large-scale phenomena and the microscopic or local phenomena, which include the flow regime, gross liquid circulation, phase holdup, interfacial phenomena, mean flow and turbulence quantities, transport coefficients, bubble rise characteristics, etc. The knowledge of these phenomena is essential for a better understanding and successful design and operation of bubble column systems. Among them, the bubble rise velocity is an important parameter characterizing the bubble behavior. Much attention has been paid to its investigation [1–3].

Most of the previous researches on the bubble rise velocity were conducted on single isolated bubbles. It is readily acknowledged that the hydrodynamic behavior of an individual bubble in a gas–liquid system generally differs from that of a single isolated bubble due to interactions with its neighboring bubbles. However, the mechanism of bubble–bubble interactions is extremely complex; a full understanding has not yet been reached. The bubbles rising in-line or the bubble chain is a specific but typical case where mutual interactions between bubbles are evident. In this particular case, the wake of the leading bubble is found to be a primary factor leading to the interactions between the trailing and leading bubbles, which could significantly change the bubble rise velocity and affect the bubble shape, bubble coalescence and breakup, and in turn affect bubble residence time, bubble size distribution, and gas–liquid interfacial area. A quantitative description of the velocity of the bubbles rising in-line could provide not only a basic understanding of the bubble–bubble interaction mechanism but also a preliminary estimation of the bubble rise velocity in general bubble column systems.

Crabtree and Bridgwater [4] measured the bubble positions and bubble coalescence time for the relative motion of two vertically aligned spherical-cap bubbles of different diameters at Reynolds numbers (*Re*) of 40–90 in a 67 wt.% solution of sucrose in water. A theory based on the wake velocity was proposed to predict the bubble coalescence time. de Nevers and Wu [5] conducted a similar study on the coalescence of spherical-cap bubbles of 1–2 cm diameters rising in glycerin and in water. A simplified model with different assumptions on the wake configurations was proposed for predicting the bubble coalescence time. Marks [6] measured the terminal velocity of air bubbles of equivalent diameters

* Corresponding author.
E-mail address: jianzhang@mail.tsinghua.edu.cn (J. Zhang).

1385-8947/02/$ – see front matter
PII: S1385-8947(02)00189-4

Nomenclature

C_d	drag coefficient of an interactive bubble
C_{d0}	drag coefficient of an isolated bubble
d	bubble diameter (m)
F_A	added mass force (N)
F_B	Basset force (N)
F_d	drag force of an interactive bubble (N)
F_{d0}	drag force of an isolated bubble (N)
F_g	buoyancy force (N)
F_j	force component of a bubble (N)
g	gravitational acceleration (m s^{-2})
p	static pressure of liquid (Pa)
Re	bubble Reynolds number based on its terminal velocity
Re_{tr}	Reynolds number of the trailing bubble
Re_0	Reynolds number of an isolated bubble
t	time (s)
t_0	reference time (s)
U	local liquid velocity (m s^{-1})
$\bar{U}$	radially averaged wake velocity over the frontal area of the trailing bubble (m s^{-1})
U_b	rise velocity of an interactive bubble (m s^{-1})
U_{b0}	rise velocity of an isolated bubble (m s^{-1})
U_0	incoming liquid velocity (m s^{-1})
x	axial coordinate, separation distance between the rear surface of the leading bubble and the frontal surface of the trailing bubble (m)
Δx	integration interval (m)

Greek letters

α, β	coefficients
μ	dynamic viscosity of liquid (kg m^{-1} s^{-1})
ν	kinematic viscosity of liquid (m^2 s^{-1})
ρ	liquid density (kg m^{-3})
ρ_b	bubble density (kg m^{-3})
τ	time (s)
$\Delta\tau$	time interval (s)

Subscript and superscript

i	difference node
$*$	non-dimensional quantity

of 0.12–1.9 cm rising in a chain through distilled water, tap water and sugar water. A model based on the turbulent wake velocity was employed to correlate the measured data. Narayanan et al. [7] measured the rise velocity of air bubble pair in aqueous glycerin solutions at *Re* of 0.5–80. Different equations which follow Stimson–Jeffery's [8] creeping flow analysis and the measured wake flow structure were developed to predict the rise velocity ratio of the bubble pair for $Re < 7$ and $Re > 7$, respectively. Omran and Foster [9] measured the terminal velocities of chains of spherical air bubbles in aqueous glycerin solutions for the ranges of $Re < 1$ and $1 < Re < 9$ and bubble diameters from 1.4 to 3 mm. In their study, Sonshine and Brenner's analysis [10] for the motion of a chain of particles at $Re < 1$ was validated and extended to the analysis of the chain motion of bubbles at $1 < Re < 9$. Bhaga and Weber [11] measured the wake velocity behind a single spherical-cap air bubble and visualized the in-line motion of two bubbles rising in aqueous sugar solutions. The rise velocity of the trailing bubble was predicted from their modified wake velocity correlation plus the bubble terminal velocity in isolation and the criterion for bubble coalescence was provided for $10 < Re < 100$. Komasawa et al. [12] investigated experimentally the dynamic behavior of a single and a pair of spherical-cap air bubbles held stationary in downward flows of deionized water and water–jelly solutions for the *Re* range of 10–10^4. The additional velocity component of the trailing bubble caused by the laminar wake of the leading bubble was found to be equal to the velocity difference between the wake and the main liquid flow. Miyahara et al. [13] studied both experimentally and analytically the velocity distribution induced in aqueous glycerin and glycerin–ethanol solutions by a chain of air bubbles, together with the shape and wake volume of the bubble chain over the range of bubble equivalent spherical diameters of 0.214–2.37 cm. The rise velocity of chain bubbles was estimated by utilizing the laminar/turbulent wake velocity and the results of drag coefficient and shape of single bubbles. Katz and Meneveau [14] visualized the motion of a train of spherical air bubbles in stagnant water at *Re* ranging from 0.2 to 35. A model based on the known flow field and wake structure around a single bubble was developed to predict the rise velocities of interactive bubble pairs.

Yuan and Prosperetti [15] numerically studied the in-line motion of two equal spherical bubbles in a viscous fluid by solving the full unsteady Navier–Stokes equations for *Re* up to 200. The detailed flow structures around the bubbles, rise velocities of the bubbles, separation distance between them, and viscous drag and potential forces acting on them were predicted. The results show that the wake of the leading bubble strongly influences the flow structure around the trailing bubble, but the leading bubble itself is little affected. The two bubbles rising in-line gradually approach and finally reach an equilibrium distance, at which the wake effect and the pressure gradient balance. The existence of such a distance is in contrast with experimental findings, which may come from assuming no bubble deformation in the numerical simulation.

The aforementioned analytical or semi analytical models for bubble motion mostly assume that the rise velocity of a bubble in a chain is the sum of the wake velocity of bubbles ahead of it and its rise velocity in isolation. Komasawa et al.'s model [12] assumes that the bubble rise velocity is equal to the main liquid velocity plus an additional velocity as indicated above, due to their downward flow and stationary bubble conditions. The model by Katz and Meneveau [14] further accounts for the effect of pressure gradients caused by the presence of neighboring bubbles on the bubble motion. It is noted that the formulations of these

models have never been rigorously derived, which hinders their general application. Also none of these models account for the acceleration effect of an interactive bubble, which could be significant for bubble–liquid systems. The present paper starts from the balance equation for the forces acting on a spherical bubble rising in a chain in liquids, based on which mathematical models for the rise velocity of an interactive bubble are derived. The semi analytical expression for the drag force ratio of an interactive sphere in intermediate *Re* range, which was developed by the authors [16], is extended to the bubble case and utilized in the model formulation. The added mass and Basset forces acting on a bubble due to its accelerated motion are taken into account in the models. The rise velocity ratios predicted by the present models are compared with the measured data of Katz and Meneveau [14].

2. Forces on an interactive bubble

Consider a two-bubble or multi-bubble system rising in-line in a quiescent liquid, as schematically shown in Fig. 1. In the analysis, it is assumed that (1) the Weber number (*We*) is much smaller than 1 where no bubble deformation occurs and the bubbles adopt a spherical shape with an identical diameter of *d*; (2) the bubble Reynolds number (*Re*) is in the order of 100 and the wake flow behind a bubble is laminar, axisymmetric, and in steady state (no wake shedding); (3) the downstream trailing bubble is located in the far wake region of the upstream leading bubble; (4) the presence of the downstream bubbles has negligible effects on the upstream flow conditions. Due to the attraction by the leading bubble wake, the trailing bubble experiences significant acceleration in its motion and finally coalesces with the leading bubble in the absence of surfactants; on the other hand, the motion of the leading bubble is almost unaffected by the trailing bubble located in its far wake region, as observed in a number of experiments mentioned previously. The forces acting on the trailing bubble during its accelerated motion are not only the drag and buoyancy as in the case of a single isolated bubble rising at its terminal velocity. Other forces, such as the inertia, pressure gradient, added mass, and Basset forces, should also be taken into account.

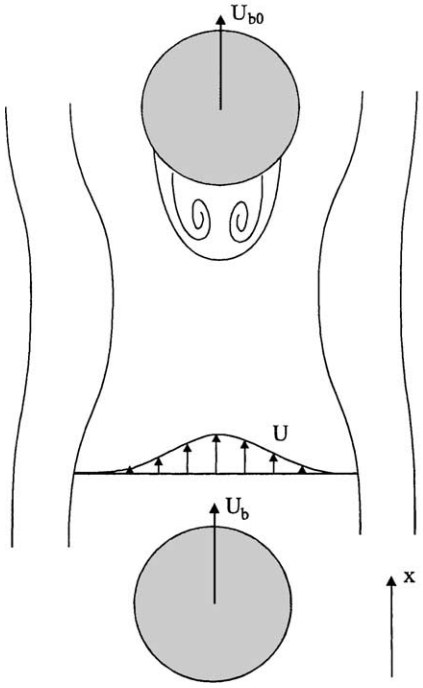

Fig. 1. Schematic flow pattern of two interactive bubbles due to wake attraction.

The balance equation for the forces acting on the trailing bubble rising in-line with the leading bubble can thus be written as

$$\frac{1}{6}\pi d^3 \rho_b \frac{dU_b}{dt} = F_g + F_d + F_p + F_A + F_B \quad (1)$$

where the terms on the right-hand side of the equation denote the buoyancy, drag, pressure gradient, added mass, and Basset forces in sequence.

As seen in Fig. 1, the positive direction of *x*-coordinate is vertically upward. The buoyancy force for the spherical bubble is expressed as

$$F_g = \tfrac{1}{6}\pi d^3(\rho - \rho_b)g \quad (2)$$

The drag force on the trailing bubble, F_d, is different from that on a single isolated bubble, F_{d0}, due to the effect of bubble wake. The local liquid velocity encountered by the trailing bubble can be equated to the radially averaged wake velocity over its exposed frontal area, $\bar{U}$, which is taken at the frontal section of the trailing bubble. The drag force of the trailing bubble can thus be written as

$$F_d = -C_d \frac{\pi}{8}\rho d^2(\bar{U} - U_b)^2 \quad (3)$$

where C_d and U_b are, respectively, the drag coefficient and rise velocity of the interactive trailing bubble. If the trailing bubble is isolated in a liquid with uniform incoming velocity of U_0, the expression for its drag force becomes

$$F_{d0} = -C_{d0} \frac{\pi}{8}\rho d^2(U_0 - U_{b0})^2 \quad (4)$$

where C_{d0} and U_{b0} are, respectively, the drag coefficient and rise velocity of a single isolated bubble. The drag force ratio, F_d/F_{d0}, is obtained from Eqs. (3) and (4) as

$$\frac{F_d}{F_{d0}} = \frac{C_d}{C_{d0}}\left(\frac{\bar{U} - U_b}{U_0 - U_{b0}}\right)^2 \quad (5)$$

The ratio of the drag coefficients, C_d/C_{d0}, is further assumed to be equal to the ratio of the *Re* of an isolated bubble to the *Re* based on the relative velocity between the local wake flow and the trailing bubble. This assumption has been verified for the case of particles aligned in tandem in a flow field

for particle Re in the order of 100 [16]. It is extended to the present case of interactive bubbles. The expression for C_d/C_{d0} is then given as

$$\frac{C_d}{C_{d0}} = \frac{Re_0}{Re_{tr}} = \frac{U_0 - U_{b0}}{\bar{U} - U_b} \tag{6}$$

where Re_0 and Re_{tr} are the Re of the isolated bubble and the trailing bubble, respectively. Substituting Eq. (6) into Eq. (5) yields

$$\frac{F_d}{F_{d0}} = \frac{\bar{U} - U_b}{U_0 - U_{b0}} \tag{7}$$

or

$$\frac{F_d}{F_{d0}} = \frac{\bar{U} - U_{b0}}{U_0 - U_{b0}} + \frac{U_{b0} - U_b}{U_0 - U_{b0}} \tag{8}$$

It is noted that $U_0 = 0$ for the present case. Employing the analytical expression for the averaged wake velocity distribution in dimensionless form [16] for the first term on the right-hand side of Eq. (8), the equation becomes

$$\frac{F_d}{F_{d0}} = \frac{U_b}{U_{b0}} - \frac{C_{d0}}{2}\left[1 - \exp\left(-\frac{Re_0 d}{16x}\right)\right] \tag{9}$$

where $Re_0 = U_{b0}d/\nu$ and x is the separation distance between the rear surface of the leading bubble and the frontal surface of the trailing bubble.

The analytical expressions for the pressure gradient, added mass and Basset forces are obtained for a single isolated bubble under the creeping flow condition. Here they are extended directly to the case of an interactive bubble at higher Re. The liquid is assumed to be pure and free of surfactants. The expressions for these forces are given, respectively, as below [17]

$$F_p = -\frac{\pi}{6}d^3\Delta p \tag{10}$$

$$F_A = \frac{\pi}{12}d^3\rho\frac{d}{dt}(U - U_b) \tag{11}$$

$$F_B = d^2\sqrt{\pi\rho\mu}\int_{t_0}^{t}\frac{d(U - U_b)/d\tau}{\sqrt{t - \tau}}\,d\tau \tag{12}$$

where d/dt denotes the substantial derivative following the bubble motion. For the present case of quiescent liquid, it is noted that $dU/dt = 0$. The trailing bubble is assumed to be located in the far wake region of the leading bubble. Over this region, the pressure gradient is negligible, i.e., $\nabla p \simeq 0$, which results in $F_p = 0$. The expressions for the added mass and Basset forces, Eqs. (11) and (12), are then reduced to

$$F_A = -\frac{\pi}{12}d^3\rho\frac{dU_b}{dt} \tag{13}$$

$$F_B = -d^2\sqrt{\pi\rho\mu}\int_{t_0}^{t}\frac{dU_b/d\tau}{\sqrt{t - \tau}}\,d\tau \tag{14}$$

Compared with the added mass force, the inertia force on the left-hand side of Eq. (1) is negligible since $\rho_b \ll \rho$ for bubble–liquid systems. Finally, the total force acting on the trailing bubble is a balance of the buoyancy, drag, added mass and Basset forces. The balance equation can be expressed as

$$\begin{aligned}\frac{1}{12}\pi d^3\rho\frac{dU_b}{dt} &= \frac{1}{6}\pi d^3\rho g + \left\{\frac{U_b}{U_{b0}} - \frac{C_{d0}}{2}\left[1 - \exp\left(-\frac{Re_0 d}{16x}\right)\right]\right\} \\ &\quad \times F_{d0} - d^2\sqrt{\pi\rho\mu}\int_{t_0}^{t}\frac{dU_b/d\tau}{\sqrt{t - \tau}}\,d\tau\end{aligned} \tag{15}$$

Note that for a single isolated bubble rising at its terminal velocity, U_{b0}, the drag force, F_{d0}, is balanced only by the buoyancy force, F_g, i.e.

$$F_{d0} = -\tfrac{1}{6}\pi d^3\rho g \tag{16}$$

Substituting Eq. (16) into Eq. (15) yields

$$\begin{aligned}\frac{dU_b}{dt} &= 2g\left\{1 - \frac{U_b}{U_{b0}} + \frac{C_{d0}}{2}\left[1 - \exp\left(-\frac{Re_0 d}{16x}\right)\right]\right\} \\ &\quad - \frac{12}{d}\sqrt{\frac{\nu}{\pi}}\int_{t_0}^{t}\frac{dU_b/d\tau}{\sqrt{t - \tau}}\,d\tau\end{aligned} \tag{17}$$

By introducing the following non-dimensional quantities

$$U_b^* = \frac{U_b}{U_{b0}}, \qquad t^* = \frac{tU_{b0}}{d}, \quad \tau^* = \frac{\tau U_{b0}}{d}, \quad x^* = \frac{x}{d} \tag{18}$$

Eq. (17) can be given in a non-dimensional form as

$$\begin{aligned}\frac{dU_b^*}{dt^*} &= \frac{2gd}{U_{b0}^2}\left\{1 - U_b^* + \frac{C_{d0}}{2}\left[1 - \exp\left(-\frac{Re_0}{16x^*}\right)\right]\right\} \\ &\quad - \frac{12}{\sqrt{\pi Re_0}}\int_{t_0^*}^{t^*}\frac{dU_b^*/d\tau^*}{\sqrt{t^* - \tau^*}}\,d\tau^*\end{aligned} \tag{19}$$

3. Models for the rise velocity of an interactive bubble

Eq. (19) provides a general differential–integral equation of motion for an interactive spherical bubble rising in-line in a quiescent liquid. Based on this equation and different assumptions for the forces acting on the bubble, different mathematical models describing the rise velocity of the trailing bubble can be derived.

Model I. The motion of the trailing bubble is assumed to be in quasi-steady state. The bubble acceleration effect in terms of the added mass and Basset forces is thus neglected. Only the wake effect is accounted for in the equation of bubble motion. The resultant equation simplified from Eq. (19) is the balance of only the buoyancy and drag forces. The rise velocity of the trailing bubble can be directly obtained as

$$U_b^* = 1 + \frac{C_{d0}}{2}\left[1 - \exp\left(-\frac{Re_0}{16x^*}\right)\right] \tag{20}$$

It is easily seen that the bubble rise velocity given in Eq. (20) is equal to the single bubble rise velocity plus the averaged liquid wake velocity. This equation is similar to those obtained by other researchers mentioned previously. It should be noted that Eq. (20) is a result of neglecting the acceleration effect of the bubble motion in the wake region.

Model II. The bubble acceleration effect is taken into account but the Basset force is assumed to be negligible for simplicity in the equation of bubble motion. The buoyancy force acting on the trailing bubble is balanced by the drag and added mass forces under this assumption. It is noted that for the in-line approaching motion of the trailing bubble towards the leading bubble, $dU_b^*/dt^* = -U_b^* dU_b^*/dx^*$. Eq. (19) is then reduced into an ordinary differential equation as given below

$$U_b^* \frac{dU_b^*}{dx^*} = \frac{2gd}{U_{b0}^2}\left\{U_b^* - 1 - \frac{C_{d0}}{2}\left[1 - \exp\left(-\frac{Re_0}{16x^*}\right)\right]\right\} \tag{21}$$

Its boundary condition is $U_b^* = 1$ at $x^* \to \infty$. Eq. (21) is numerically solved using a finite difference method to yield the bubble rise velocity, U_b^*, varying with the separation distance between the two bubbles, x^*.

Model III. Both the wake effect and the bubble acceleration effect including the added mass and Basset forces are taken into account in the model. The equation of bubble motion, i.e., Eq. (19), can be rewritten as

$$U_b^* \frac{dU_b^*}{dx^*} = \frac{2gd}{U_{b0}^2}\left\{U_b^* - 1 - \frac{C_{d0}}{2}\left[1 - \exp\left(-\frac{Re_0}{16x^*}\right)\right]\right\} + \frac{12}{\sqrt{\pi Re_0}}\int_{t_0^*}^{t^*} \frac{dU_b^*/d\tau^*}{\sqrt{t^* - \tau^*}}\, d\tau^* \tag{22}$$

which satisfies the boundary conditions: $U_b^* = 1$ and $dU_b^*/dx^* = 0$ at $x^* \to \infty$. The finite difference method is utilized to numerically solve Eq. (22). The term on the left-hand side of Eq. (22) is discretized by the following first-order difference scheme:

$$\left(\frac{dU_b^*}{dx^*}\right)_i = \frac{U_{b,i}^* - U_{b,i-1}^*}{\Delta x_i^*} \tag{23}$$

where $\Delta x_i^* = x_i^* - x_{i-1}^*$. The Basset force term on the right-hand side of Eq. (22) is numerically integrated by the Euler formula. To avoid singularity of the integrand at $\tau^* = t_i^*$, the value of the integrand at any time interval $\Delta\tau_k^*$ ($= t_k^* - t_{k-1}^*$, $k = 1, 2, \ldots, i$) is evaluated at $\tau^* = t_{k-1}^*$. Thus the Basset force term can be explicitly calculated in the resultant difference equation, which is given as below

$$U_{b,i}^* \frac{U_{b,i}^* - U_{b,i-1}^*}{\Delta x_i^*} - \frac{2gd}{U_{b0}^2} U_{b,i}^* = -\frac{2gd}{U_{b0}^2}\left\{1 + \frac{C_{d0}}{2}\left[1 - \exp\left(-\frac{Re_0}{16x^*}\right)\right]\right\} + \frac{12}{\sqrt{\pi Re_0}}\int_{t_0^*}^{t_i^*} \frac{dU_b^*/d\tau^*}{\sqrt{t_i^* - \tau^*}}\, d\tau^* \tag{24}$$

$U_{b,i}^*$ can be solved from Eq. (24) and given in an explicit form as

$$U_{b,i}^* = 0.5\left(\alpha + \sqrt{\alpha^2 - 4\beta}\right) \tag{25}$$

where

$$\alpha = U_{b,i-1}^* + \Delta x_i^* \frac{2gd}{U_{b0}^2} \tag{26}$$

and

$$\beta = \Delta x_i^* \frac{2gd}{U_{b0}^2}\left\{1 + \frac{C_{d0}}{2}\left[1 - \exp\left(-\frac{Re_0}{16x^*}\right)\right]\right\} - \Delta x_i^* \frac{12}{\sqrt{\pi Re_0}}\int_{t_0^*}^{t_i^*} \frac{dU_b^*/d\tau^*}{\sqrt{t_i^* - \tau^*}}\, d\tau^* \tag{27}$$

To minimize numerical errors caused by the first-order difference scheme and the Euler integration formula, sufficiently fine integration intervals (Δx_i^*) are adopted in the calculation. The obtained results should not dependent on the specific integration intervals.

4. Results and discussion

To validate the mathematical models proposed above, the ratios of the rise velocity of the trailing bubble to that of an isolated bubble which vary with the separation distance between the leading and trailing bubbles are calculated by Models I–III. The obtained results are compared with the experimental data of Katz and Meneveau [14]. Their data were measured from spherical air bubble pairs rising in distilled water at small Eötvös numbers ($Eo < 0.3$). The wall effects are negligible for their measurements since the bubble sizes are much smaller than the chamber width. The model calculations are conducted for three cases of bubble pair motion at *Re* of 35.4, 21.5 and 3.06, which are identical to the experimental conditions. The spherical bubble diameters, *d*, for these three cases are 475, 349 and 158 μm, respectively. The corresponding single bubble rise velocities, U_{b0}, were measured to be 75, 62 and 19.5 m s^{-1}, respectively. Based on the relationship, $C_{d0} = 4gd/3U_{b0}^2$, and these data, the drag coefficients of the single isolated bubbles are obtained as 1.10, 1.19 and 5.43 for the three cases, respectively. The above data for U_{b0} and C_{d0} are used in the present model calculation.

Figs. 2–4 show the variations of the rise velocity ratio of the trailing bubble with the separation distance calculated by Models I–III at *Re* of 35.4, 21.5 and 3.06, respectively. The measured data of Katz and Meneveau [14] are also presented in these figures for comparison. Models II and III are calculated using the finite difference method described above. Equal dimensionless integration intervals (Δx_i^*) of both 0.05 and 0.025 are adopted in the calculations. The differences between the results for these two integration intervals are found to be minor. The results reported here are

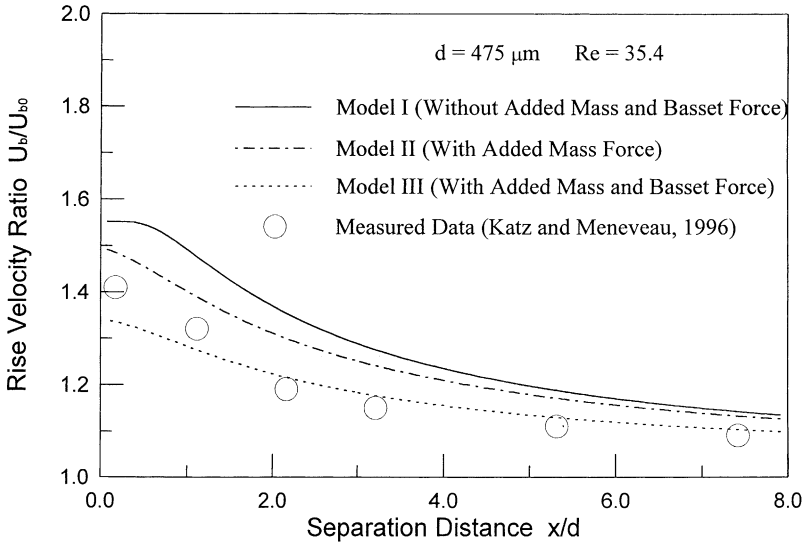

Fig. 2. Rise velocity ratio of the trailing bubble of $d = 475\,\mu m$.

those for the integration interval $\Delta x_i^* = 0.05$. Although the models are valid only in the far wake region of the leading bubble ($x^* > 2$), the calculations are still extended to the near wake region of the leading bubble where the pressure gradient force should not be neglected. The calculated results for the whole wake region are presented in the figures.

As shown in Figs. 2–4, all the three models can predict the general trend of the rise velocity of the trailing bubble varying with the separation distance between the two bubbles. The rise velocity of the trailing bubble increases with decreasing bubble separation distance. It is always larger than the rise velocity of a single isolated bubble due to the wake attraction. However, the discrepancies between the predictions via Model I and the measured data are evident. It is seen that Model I overestimates the rise velocity of the trailing bubble in comparison with the test data. This result is deemed due to the neglect of the bubble acceleration effect. Thus Model I, which has been commonly used in the aforementioned literature and accounts for the wake effect only, can be utilized only as a first-order approximation for the rise velocity of the trailing bubble. Nevertheless, this model is easy for engineering applications due to simplicity of the form.

For achieving a better prediction of the rise velocity of the trailing bubble, the bubble acceleration effect should be taken into account. Model II incorporates the wake effect and the added mass force, the latter accounts for part of the acceleration effect. It is seen from Figs. 2–4 that the predictions with Model II are improved over those with

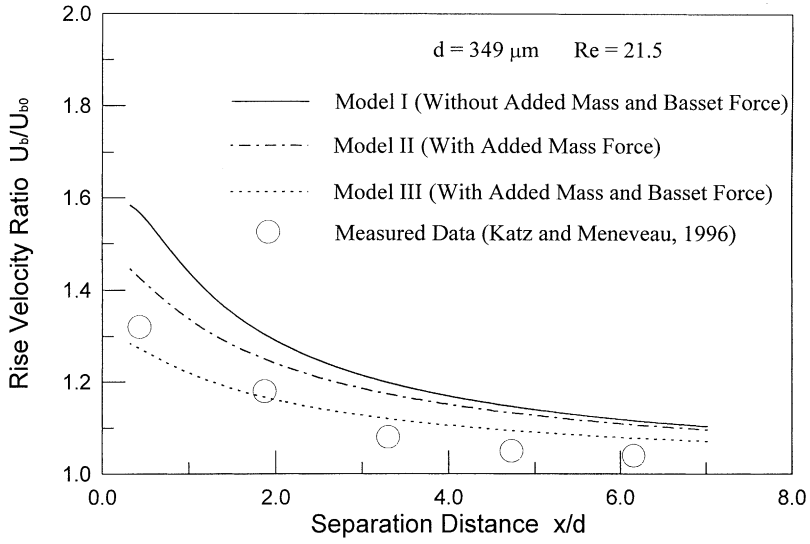

Fig. 3. Rise velocity ratio of the trailing bubble of $d = 349\,\mu m$.

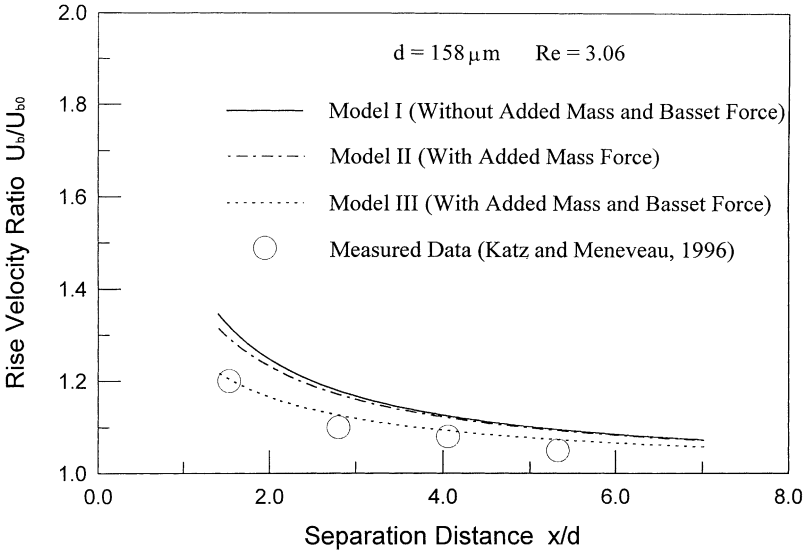

Fig. 4. Rise velocity ratio of the trailing bubble of $d = 158\,\mu m$.

Model I and the former are closer to the measured data than the latter. The improvement is more obvious as the separation distance between the bubbles decreases. It is also more evident for the bubbles of larger diameters. However, the discrepancies between the predictions and the measured data still exist for Model II, as seen in the figures.

As shown in Figs. 2–4, the best agreement between the prediction and the measured data is achieved with Model III, which accounts for both the wake effect and the bubble acceleration effect including the added mass and Basset forces. The agreement even extends to the near wake region of the leading bubble and beyond the scope where the model assumptions are valid, as seen in Figs. 2 and 3. The improvement of Model III over Models I and II in predicting the rise velocity of the trailing bubble is more evident for larger bubbles and smaller separation distances. The results shown here indicate that the wake effect as well as the bubble acceleration effect should be take into account to properly describe the in-line motion of the trailing bubble in the far wake region of the leading bubble. Both the added mass force and the Basset force are not negligible and are important for describing the accelerated motion of bubbles in liquids.

Fig. 5 shows the drag, added mass, and Basset forces for the trailing bubble of diameter of 349 μm, varying with the separation distance between the two bubbles. The forces shown in the figure are calculated based on Model III and

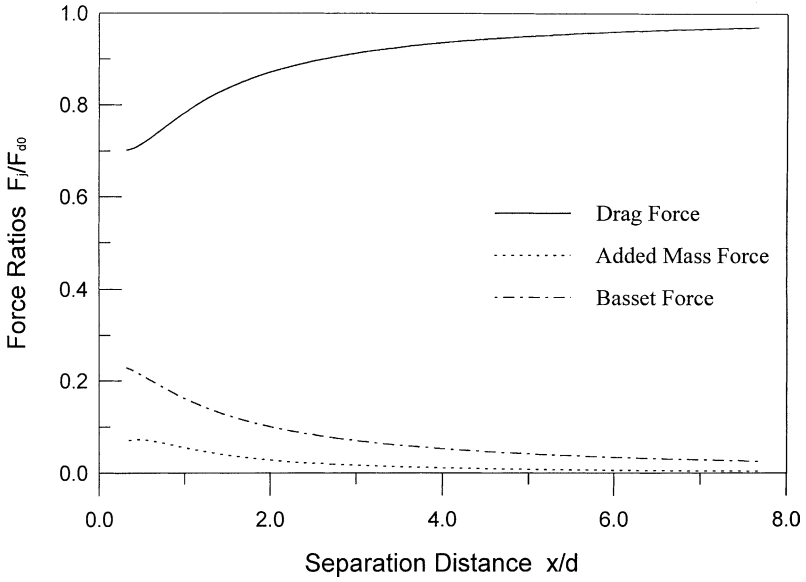

Fig. 5. Drag, added mass and Basset forces of the trailing bubble of $d = 349\,\mu m$.

are non-dimensionalized by the drag force of the single isolated bubble of the same diameter. It is seen that the drag force decreases with decreasing bubble separation distance, whereas both the added mass force and the Basset force increase with decreasing separation distance. Although the total resistant force on the trailing bubble, which is the sum of the drag, added mass and Basset forces, remains constant during its motion, the reduction in the drag force as the trailing bubble approaches the leading bubble is predicted by the present model. As seen in Fig. 5, the drag, added mass, and Basset forces take up about 87, 3 and 10% of the total resistant force, respectively, at the separation distance $x^* = 2$. This result indicates that even though the drag force dominates the total resistance force for the bubble accelerated motion, the added mass and Basset forces should not be neglected in the far wake region of the leading bubble. One possible reason responsible for this is that the density ratio of liquid to bubble is high for bubble–liquid systems.

5. Concluding remarks

Three mathematical models for predicting the in-line rise velocity of an interactive spherical bubble in the *Re* range in the order of 100 [*Re* ∼O(100)] are developed, based on different assumptions for the balance equation of the forces acting on the bubble. A comparison of the predicted results by the three models with the measured data shows that the general trend of the rise velocity of the trailing bubble increasing with decreasing bubble separation distance can be predicted by these models. However, the predictions by Model I can be used only as an estimation of the rise velocity of the trailing bubble. Models II and III improve the predictions over Model I. The predictions by Model III are found to agree best with the measurements among the three models. The present results indicate that both the wake effect and the bubble acceleration effect should be taken into account in analyzing the motion of the trailing bubble in the far wake region of the leading bubble. The added mass and Basset forces are not negligible for the accelerated motion of bubbles in liquids.

References

[1] R. Clift, J.R. Grace, M.E. Weber, Bubbles, Drops and Particles, Academic Press, New York, 1978.
[2] D. Bhaga, M.E. Weber, Bubbles in viscous liquids: shapes, wakes and velocities, J. Fluid Mech. 105 (1981) 61–85.
[3] L.-S. Fan, K. Tsuchiya, Bubble Wake Dynamics in Liquids and Liquid–Solid Suspensions, Butterworth-Heinemann, Stoneham, MA, 1990.
[4] J.R. Crabtree, J. Bridgwater, Bubble coalescence in viscous liquids, Chem. Eng. Sci. 26 (1971) 839–851.
[5] N. de Nevers, J.-L. Wu, Bubble coalescence in viscous fluids, AIChE J. 17 (1971) 182–186.
[6] C.H. Marks, Measurements of the terminal velocity of bubbles rising in a chain, ASME J. Fluids Eng. 95 (1973) 17–22.
[7] S. Narayanan, L.H.J. Goossens, N.W.F. Kossen, Coalescence of two bubbles rising in line at low Reynolds numbers, Chem. Eng. Sci. 29 (1974) 2071–2082.
[8] M. Stimson, G.B. Jeffery, The motion of two spheres in a viscous fluid, Proc. Roy. Soc. London A 111 (1926) 110–116.
[9] N.M. Omran, P.J. Foster, The terminal velocity of a chain of drops or bubbles in a liquid, Trans. Inst. Chem. Eng. 55 (1977) 171–177.
[10] R.M. Sonshine, H. Brenner, The Stokes translation of two or more particles along the axis of an infinitely long circular cylinder, Appl. Sci. Res. 16 (1966) 425–454.
[11] D. Bhaga, M.E. Weber, In-line interaction of a pair of bubbles in a viscous liquid, Chem. Eng. Sci. 35 (1980) 2467–2474.
[12] I. Komasawa, T. Otake, M. Kamojima, Wake behavior and its effect on interaction between spherical-cap bubbles, J. Chem. Eng. Jpn. 13 (1980) 103–109.
[13] T. Miyahara, S. Kaseno, T. Takahashi, Studies on chain of bubbles rising through quiescent liquid, Can. J. Chem. Eng. 62 (1984) 186–193.
[14] J. Katz, C. Meneveau, Wake-induced relative motion of bubbles rising in line, Int. J. Multiphase Flow 22 (1996) 239–258.
[15] H. Yuan, A. Prosperetti, On the in-line motion of two spherical bubbles in a viscous fluid, J. Fluid Mech. 278 (1994) 325–349.
[16] J. Zhang, L.-S. Fan, A semi analytical expression for the drag force of an interactive particle due to wake effect, Ind. Eng. Chem. Res., in press.
[17] F.A. Morrison Jr., M.B. Stewart, Small bubble motion in an accelerating liquid, ASME J. Appl. Mech. 43 (1976) 399–403.